New Phytologist Supporting Information
Leaf gas exchange measurements for steady-state stomatal conductance model calibration

Kyle T. Rizzo[a], Tong Lei[a], Thomas N. Buckley[a], Brian N. Bailey[a,*]

[a]*Department of Plant Sciences, University of California, Davis, Davis, CA USA 95616*

[*]Corresponding author. *Email address*: bnbailey@ucdavis.edu (Brian Bailey)

Article acceptance date: 22 December 2025

Notes S1. Estimation of Net Photosynthesis with a Porometer and Farquhar-von Caemmerer-Berry Model Parameters

The Ball-Woodrow-Berry (1987), Ball-Berry-Leuning (1995), and Medlyn et al. (2011) stomatal conductance models, along with many others, treat assimilation (A) as a model input. Porometers provide a quick measurement of stomatal conductance and environmental conditions, but lack a measurement of A. However, an inversion approach to solve for internal leaf CO_2 and A given porometer measurements and previously estimated Farquhar-von Caemmerer-Berry photosynthetic (FvCB) model parameters *(Farquhar et al., 1980)* is possible.

Given a porometer measurement with stomatal conductance (g_{sw}), incident leaf PAR (Q), leaf temperature (T_L), and using the FvCB photosynthesis model $A_{FvCB}(C_i, Q, T, \mathrm{P})$ parameterized with species specific parameters, P, we solve for the internal CO_2 concentration (C_i) that balances net assimilation and Fickian diffusion into the leaf from the atmosphere:

$$F(C_i) = A_{FvCB}(C_i, Q, T, \mathrm{P}) - g_{sw} \cdot (C_a - C_i) = 0. \quad (1)$$

Mesophyll conductance is assumed non-limiting (infinite) and atmospheric CO_2 concentration (C_a) is assumed to be 420 μmol mol^{-1}. The equation solving was performed numerically using MATLAB's `vpasolve`. A complete description of the $A_{FvCB}(C_i, Q, T, \mathrm{P})$ used here can be found in *(Lei et al., 2025)*.

Table S1. Extracted Farquhar, von Caemmerer, Berry model parameters of walnut (Juglans regia) used in this study. Input data was fit using PhoTorch (Lei et al., 2025) and consisted of 12 Dynamic Assimilation™ Technique A-C_i (LI-6800, LI-COR Biosciences, NE, USA) response curves across a range of cuvette light setpoints from 0-2000 μmol m^{-2} s^{-1} and cuvette air temperatures from 25-40 °C. Fixed parameter values were obtained from Bernacchi et al. (2001) and Sharkey et al. (2007).

Parameter	Value	Fit or Fixed	Description	Units
V_{cmax25}	81.6	fit	max carboxylation rate (Rubisco)	μmol m^{-2} s^{-1}
J_{max25}	201.9	fit	max electron transport rate (RuBP regeneration)	μmol m^{-2} s^{-1}
TPU_{25}	10.2	fit	triose-phosphate utilization rate	μmol m^{-2} s^{-1}
R_{d25}	0.9	fit	mitochondrial respiration rate	μmol m^{-2} s^{-1}
α	0.362	fit	quantum efficiency (light response initial slope)	μmol μmol^{-1}
θ	0	fit	light response curvature	–
$\Gamma^*{}_{25}$	42.23	fixed	photorespiratory CO_2 compensation point	μmol mol^{-1}
K_{c25}	384.7	fixed	Michaelis-Menten constant of Rubisco for CO_2	μmol mol^{-1}
K_{o25}	272.7	fit	Michaelis-Menten constant of Rubisco for O_2	mmol mol^{-1}
O	213.5	fixed	O_2 concentration	mmol mol^{-1}
g_m	∞	fixed	mesophyll conductance	mol m^{-2} s^{-1}
α_g	0.000	fixed	fraction of photorespiratory glycolate recycling	–
$T_{opt,Vcmax}$	316.5	fit	optimum temperature of V_{cmax}	K
$T_{opt,Jmax}$	308.6	fit	optimum temperature of J_{max}	K
$T_{opt,TPU}$	310.4	fit	optimum temperature of TPU	K
$\Delta H_{a,Vcmax}$	85.3	fit	activation enthalpy of V_{cmax}	kJ mol^{-1}
$\Delta H_{a,Jmax}$	41.4	fit	activation enthalpy of J_{max}	kJ mol^{-1}
$\Delta H_{a,TPU}$	21.9	fit	activation enthalpy of TPU	kJ mol^{-1}
$\Delta H_{a,Rd}$	46.4	fit	activation enthalpy of R_d	kJ mol^{-1}
$\Delta H_{a,\Gamma^*}$	37.83	fixed	activation enthalpy of Γ^*	kJ mol^{-1}
$\Delta H_{a,Kc}$	79.43	fixed	activation enthalpy of K_c	kJ mol^{-1}
$\Delta H_{a,Ko}$	36.38	fixed	activation enthalpy of K_o	kJ mol^{-1}
$\Delta H_{d,Vcmax}$	500.6	fit	deactivation enthalpy of V_{cmax}	kJ mol^{-1}
$\Delta H_{d,Jmax}$	308.2	fit	deactivation enthalpy of J_{max}	kJ mol^{-1}
$\Delta H_{d,TPU}$	434.9	fit	deactivation enthalpy of TPU	kJ mol^{-1}

Species represented in this study are listed in the following table.

Table S2. Species used in the study.

Common Name	Latin Name	Response State	Figure
Apple	*Malus domestica*	steady	2
Ash	*Fraxinus americana*	steady	2
Big Leaf Maple	*Acer macrophyllum*	steady	2
Cherry	*Prunus avium*	steady	2
Texas Red Oak	*Quercus buckleyi*	steady	2,5,9
Pear	*Pyrus communis*	steady	2
Prune	*Prunus domestica*	steady	2
Almond	*Prunus dulcis*	both	2
Cowpea	*Vigna unguiculata*	both	2,3
Eastern Redbud	*Cercis canadensis*	both	2,4,6,8,10
Pistachio	*Pistacia vera*	both	2
Walnut	*Juglans regia*	both	2,3,7
Western Redbud	*Cercis occidentalis*	both	2,3
Blue Elderberry	*Sambucus nigra* ssp. *caerulea*	non-steady	2
California Bay Laurel	*Umbellularia californica*	non-steady	2
Grape	*Vitis vinifera*	non-steady	2
Olive	*Olea europaea*	non-steady	2
Toyon	*Heteromeles arbutifolia*	non-steady	2

Notes S2. Nonlinear Mixed-Effects Modeling

For datasets with known leaf identification (repeated survey of tagged leaves, and steady-state IRGA measurements), we used nonlinear mixed-effects (NLME) modeling to identify population level parameters and individual leaf parameters. The general stomatal model formulation was

$$g_{sw,ij} = f\left(\mathrm{x}_{ij}, \mathrm{P} + \mathrm{p}_i\right) + \epsilon_{ij}, \tag{2}$$

where $g_{sw,ij}$ is the j^{th} stomatal conductance observation on the i^{th} leaf, x_{ij} are the environmental input variables for each observation, P is the population-level parameters (fixed effects), p_i are the i^{th} leaf parameter deviations (random effects), and ϵ_{ij} is the residual error.

Parameters for the nonlinear mixed-effects model were estimated using MATLAB's `nlmefit` function, while the unlabeled, random canopy survey, parameters were fit using `lsqcurvefit`. For the Ball-Berry-Leuning model, Γ was fixed to alleviate numerical instabilities in `nlmefit`.

The marginal R^2 represents the goodness of fit of the fixed effects alone, or the population-level parameters, and is calculated as

$$R_m^2 = 1 - \frac{\sum_{i,j}(g_{sw,ij} - f(\mathrm{x}_{ij},\mathrm{P}))^2}{\sum_{i,j}(g_{sw,ij} - \bar{g}_{sw})^2}. \quad (3)$$

The conditional R^2, on the other hand, represents the goodness of fit of both the fixed and random effects, where each leaf has some normally distributed set of unique parameters around the shared set of fixed effect, population-level parameters. It is calculated as

$$R_c^2 = 1 - \frac{\sum_{i,j}(g_{sw,ij} - f(\mathrm{x}_{ij},\mathrm{P} + \mathrm{p}_i))^2}{\sum_{i,j}(g_{sw,ij} - \bar{g}_{sw})^2}. \quad (4)$$

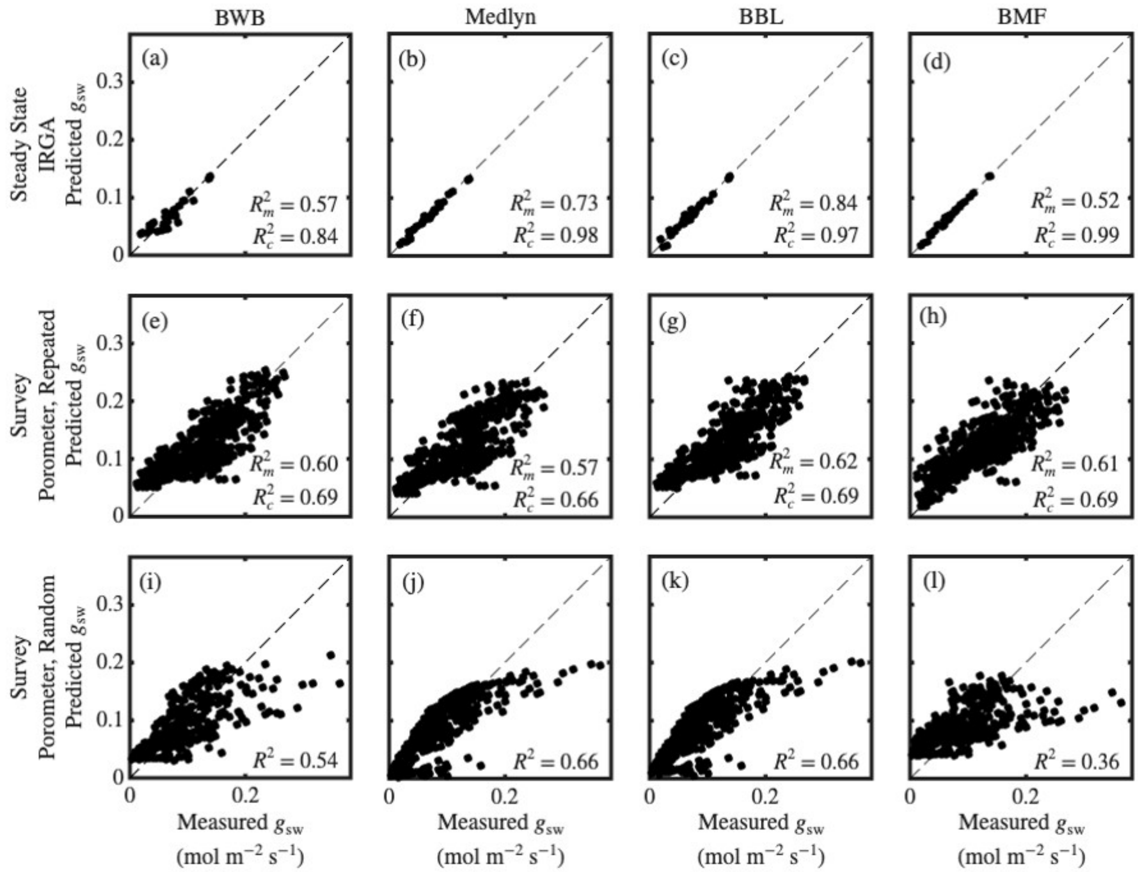

Figure S1. Stomatal conductance model fit results across 3 measurement collection methods: steady-state with an infrared gas analyzer (IRGA), repeated diurnal survey of tagged leaves with a porometer, and random diurnal survey of the canopy with a porometer. Models used are Ball-Woodrow-Berry 1987 (BWB), Medlyn et al. 2011 (MED), Ball-Berry-Leuning 1995 (BBL), and Buckley-Turnbull-Adams 2012 (BTA). Nonlinear mixed-effects modeling was used for steady-state and repeated porometry groups. R_m^2 is the marginal coefficient of determination, denoting the fit of the population level (fixed effect) fit of the models to the data, and R_c^2 is the conditional R^2, denoting the fit of individual leaf-level parameters (fixed plus random effects). Random porometry excludes leaf-level identification and shows only the population-level R^2.

Table S3. Ball-Berry-Woodrow (1987) stomatal conductance (gsw) model fitting results. A nonlinear mixed effects model approach was used on leaves of Walnut (Juglans regia). Results are displayed for randomly surveyed leaves with a porometer (P), tagged and repeatedly surveyed leaves with a porometer (P), and leaves measured in steady-state with an IRGA (I).

$g_{sw} = g_0 + g_1 \frac{Ah}{C_a}$	g_0	g_1	R^2
Aggregate Parameters			
Random Survey (P)	0.0328	5.37	0.538
Tagged Survey (P) Fixed	0.0716	6.02	0.596[m]
Steady State (I) Fixed	0.0338	4.11	0.566[m]
Tagged Survey (P) - Mixed Effects Model (8 leaves)			
Fixed Effects	0.0716	6.02	--
SD of Random Effects	0.0144	1.14	--
Marginal R^2	--		0.596
Conditional R^2	--		0.686
Individual leaves			
Leaf P1	0.0739	6.60	0.671
Leaf P2	0.0702	3.71	0.632
Leaf P3	0.0858	5.29	0.217
Leaf P4	0.0956	5.94	0.277
Leaf P5	0.0602	6.76	0.744
Leaf P6	0.0710	6.10	0.805
Leaf P7	0.0663	6.89	0.741
Leaf P8	0.0494	6.92	0.804
Steady State (I) - Mixed Effects Model (6 leaves)			
Fixed Effects	0.0338	4.11	--
SD of Random Effects	0.0000	1.43	--
Marginal R^2	--		0.566
Conditional R^2	--		0.840
Individual leaves			

Leaf I1	0.0338	2.59	0.305
Leaf I2	0.0338	4.18	0.455
Leaf I3	0.0338	4.70	0.885
Leaf I4	0.0338	6.54	0.830
Leaf I5	0.0338	3.79	0.679
Leaf I6	0.0338	2.85	0.552

[m] Marginal R^2 (fixed effects only)

P = Porometer, I = IRGA

Table S4. Medlyn et al. (2011) stomatal conductance (gsw) model fitting results. A nonlinear mixed effects model approach was used on leaves of Walnut (Juglans regia). Results are displayed for randomly surveyed leaves with a porometer (P), tagged and repeatedly surveyed leaves with a porometer (P), and leaves measured in steady-state with an IRGA (I).

$g_0 + 1.6(1 + \frac{g_1}{\sqrt{VPD}})\frac{A}{C_a}$	g_0	g_1	R^2
Aggregate Parameters			
Random Survey (P)	0.0048	1.36	0.663
Tagged Survey (P) Fixed	0.0667	0.75	0.572[m]
Steady State (I) Fixed	0.0153	1.08	0.734[m]
Tagged Survey (P) - Mixed Effects Model (8 leaves)			
Fixed Effects	0.0667	0.75	--
SD of Random Effects	0.0192	0.65	--
Marginal R^2	--		0.572
Conditional R^2	--		0.663
Individual leaves			
Leaf P1	0.0637	1.44	0.723
Leaf P2	0.0598	0.22	0.566
Leaf P3	0.0904	-0.21	0.189
Leaf P4	0.0993	0.00	0.226
Leaf P5	0.0558	1.39	0.772
Leaf P6	0.0672	0.88	0.771

Leaf P7	0.0586	0.96	0.690
Leaf P8	0.0390	1.35	0.735
Steady State (I) - Mixed Effects Model (6 leaves)			
Fixed Effects	0.0153	1.08	--
SD of Random Effects	0.0000	0.63	--
Marginal R^2	--		0.734
Conditional R^2	--		0.980
Individual leaves			
Leaf I1	0.0153	0.26	0.923
Leaf I2	0.0153	1.10	0.919
Leaf I3	0.0153	1.39	0.941
Leaf I4	0.0153	2.12	0.986
Leaf I5	0.0153	1.18	0.958
Leaf I6	0.0153	0.40	0.977

^{m} Marginal R^2 (fixed effects only)

P = Porometer, I = IRGA

Table S5. Ball-Berry-Leuning (1995) stomatal conductance (gsw) model fitting results. A nonlinear mixed effects model approach was used on leaves of Walnut (Juglans regia). Results are displayed for randomly surveyed leaves with a porometer (P), tagged and repeatedly surveyed leaves with a porometer (P), and leaves measured in steady-state with an IRGA (I).

$g_{sw} = g_0 + \frac{A}{C_a - \Gamma}(1 + \frac{VPD}{VPD_0})^{-1}$	g_0	g_1	VPD_0	Γ	R^2
Aggregate Parameters					
Random Survey (P)	0.0094	3.53	7.86	42.8*	0.661
Tagged Survey (P) Fixed	0.0659	11.43	0.51	42.8*	0.620^m
Steady State (I) Fixed	0.0155	3.19	7.81	42.8*	0.743^m
Tagged Survey (P) - Mixed Effects Model (8 leaves)					
Fixed Effects	0.0659	11.43	0.51	42.8*	--
SD of Random Effects	0.0122	0.00	0.10	--	--

Marginal R^2		--		--	0.620
Conditional R^2		--		--	0.694
Individual leaves					
Leaf P1	0.0673	11.43	0.53	42.8*	0.771
Leaf P2	0.0632	11.43	0.32	42.8*	0.718
Leaf P3	0.0771	11.43	0.45	42.8*	0.253
Leaf P4	0.0864	11.43	0.52	42.8*	0.357
Leaf P5	0.0572	11.43	0.52	42.8*	0.778
Leaf P6	0.0661	11.43	0.50	42.8*	0.782
Leaf P7	0.0628	11.43	0.58	42.8*	0.733
Leaf P8	0.0473	11.43	0.63	42.8*	0.758
Steady State (I) - Mixed Effects Model (6 leaves)					
Fixed Effects	0.0155	3.19	7.81	42.8*	--
SD of Random Effects	0.0000	0.72	0.00	--	--
Marginal R^2		--		--	0.743
Conditional R^2		--		--	0.979
Individual leaves					
Leaf I1	0.0155	2.27	7.81	42.8*	0.888
Leaf I2	0.0155	3.21	7.81	42.8*	0.912
Leaf I3	0.0155	3.54	7.81	42.8*	0.952
Leaf I4	0.0155	4.39	7.81	42.8*	0.986
Leaf I5	0.0155	3.29	7.81	42.8*	0.961
Leaf I6	0.0155	2.42	7.81	42.8*	0.967

* Fixed parameter

m Marginal R^2 (fixed effects only)

P = Porometer, I = IRGA

Table S6. Buckley-Turnbull-Adams (2012) stomatal conductance (gsw) model fitting results. A nonlinear mixed effects model approach was used on leaves of Walnut (Juglans regia). Results are displayed for randomly surveyed leaves with a porometer (P), tagged and repeatedly surveyed leaves with a porometer (P), and leaves measured in steady-state with an IRGA (I).

$g_{sw} = \dfrac{E_m(Q+i_0)}{k+bQ+(Q+i_0)D}$	E_m	i_0	k	b	R^2
Aggregate Parameters					
Random Survey (P)	5.48	291.4	29829	0.0000	0.363
Tagged Survey (P) Fixed	9.75	3.7	3597	31.3212	0.611 m
Steady State (I) Fixed	3.19	196.3	30992	0.5116	0.524 m
Tagged Survey (P) - Mixed Effects Model (8 leaves)					
Fixed Effects	9.75	3.7	3597	31.3212	--
SD of Random Effects	1.00	5.7	0	2.3066	--
Marginal R^2			--		0.611
Conditional R^2			--		0.689
Individual leaves					
Leaf P1	10.20	-2.6	3597	30.2284	0.869
Leaf P2	7.73	5.0	3597	32.7850	0.661
Leaf P3	9.48	8.7	3597	32.3013	0.164
Leaf P4	11.12	10.5	3597	30.6156	0.400
Leaf P5	9.76	2.1	3597	31.7158	0.908
Leaf P6	9.86	5.8	3597	31.4860	0.773
Leaf P7	10.13	0.6	3597	31.3304	0.728
Leaf P8	9.75	-0.7	3597	30.1068	0.563
Steady State (I) - Mixed Effects Model (6 leaves)					
Fixed Effects	3.19	196.3	30992	0.5116	--
SD of Random Effects	0.00	123.8	16492	2.9272	--
Marginal R^2			--		0.524
Conditional R^2			--		0.991
Individual leaves					
Leaf I1	3.19	339.9	47225	2.5027	0.889
Leaf I2	3.19	277.2	26254	0.9408	0.984
Leaf I3	3.19	132.8	14377	2.2217	0.987

Leaf I4	3.19	12.0	8124	-3.9887	0.999
Leaf I5	3.19	192.6	47861	0.6336	0.982
Leaf I6	3.19	223.5	42108	0.7596	0.971

[m] Marginal R^2 (fixed effects only)

P = Porometer, I = IRGA

Notes S3. 3D modeling framework description

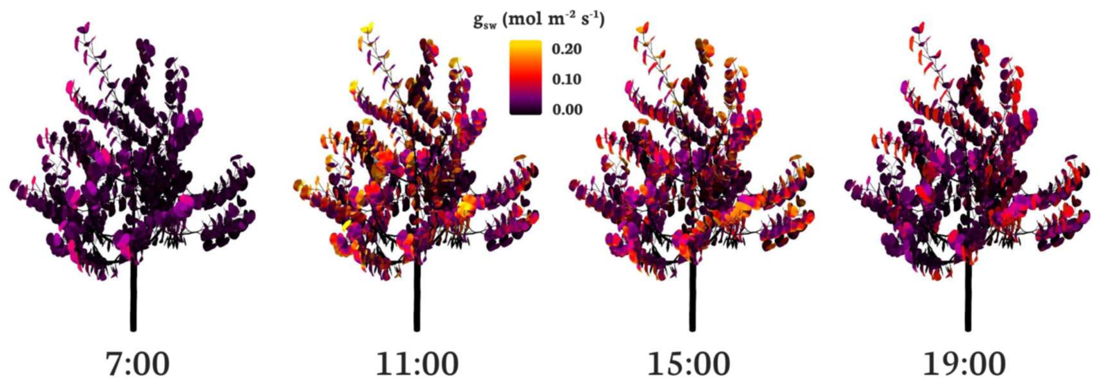

Figure S2. Snapshots in time (PST) of an eastern redbud (Cercis canadensis) model in the plant simulation library Helios, colored by stomatal conductance (g_{sw}; mol m^{-2} s^{-1}). The Buckley, Turnbull, Adams (2012) stomatal conductance model was used, with coefficients E_m = 21.88, i_0 = 11.47, k = 138700, b = 0. Environmental conditions were set from the June 4, 2024 CIMIS weather data provided from the Davis, CA, USA station.

To simulate stomatal dynamics in a tree canopy, a biophysical plant modeling framework (Bailey, 2019) was used to couple light, heat, and water exchange on a 3D canopy mesh. Light interception of PAR (≲ 700 nm), NIR (≳ 700 nm), and longwave (sky and terrestrial emission) is simulated with a reverse ray-tracing approach (Bailey, 2018). Following incident light simulation, temperatures are computed by updating temperatures through an implicit backward Euler scheme of a non-steady-state surface energy balance of the form

$$T_s^{t+1} = T_s^t + \frac{\Delta t}{C_p}\left(R_s - \epsilon\sigma(T_s^{t+1})^4 - c_p\phi g_{bw}(T_s^{t+1} - T_a) - \lambda_w g_{tw}\frac{e_s(T_s^{t+1}) - e_s(T_a)h_a}{P_a}\right), \quad (5)$$

with

$$g_{tw} = \frac{g_{bw}g_{sw}}{g_{bw} + g_{sw}}, \quad (6)$$

and

$$e_s(T) = a \cdot \exp\left[\frac{bT}{c + T}\right], \tag{7}$$

with coefficients $a = 611$ Pa, $b = 17.502$ °C^{-1}, $c = 240.97$ °C, and T specified in degrees Celsius (Tetens, 1930). T_s is the surface temperature (K) with superscript denoting the time index, incremented with a timestep of Δt; all other variables are at the time index being solved for, t+1. R_s is the total all-wave radiation absorbed by the surface (W m^{-2}), ϵ is the surface emissivity (-), σ is the Stefan-Boltzmann constant (W m^{-2} K^{-4}), C_p is the heat capacity of the object on a surface area basis (J m^{-2} K^{-1}), c_p is the heat capacity of air (J mol^{-1} K^{-1}), ϕ is the empirical diffusivity ratio of heat to water vapor (-), λ_w is the latent heat of vaporization of water vapor (J mol^{-1}), g_{tw} is the total conductance to water vapor (mol m^{-2} s^{-1}), g_{bw} is the boundary layer conductance to water vapor (mol m^{-2} s^{-1}), g_{sw} is the stomatal conductance to water vapor (mol m^{-2} s^{-1}), $e_s(T)$ is the saturation vapor pressure function of temperature (Pa), T_a is the air temperature (K), h_a is the air relative humidity (-), and P_a is the atmospheric pressure (Pa). For the redbud simulation, a C_p for leaves of 1114 J m^{-2} K^{-1} (Buckley et al., 2023), c_p of 29.25 J mol^{-1} K^{-1}, λ_w of 44000 J mol^{-1}, and ϕ of 1.08 was used. A Newton-Raphson iteration method is used to solve Eqn. 5 for T_s^{t+1}.

Boundary layer conductance differs with primitive type in the simulation. For leaves, the Pohlhausen equation was used

$$g_{bw} = \frac{0.135}{\phi}\sqrt{\frac{U}{L}}, \tag{8}$$

where U is the bulk wind speed (m s^{-1}), and L is the leaf length (m). For ground primitives, boundary layer conductance to heat (ϕg_{bw}) is computed following (Kustas and Norman, 1999) as

$$\phi g_{bw} = 0.166 + 0.5U. \tag{9}$$

Stomatal conductance is modeled with the Buckley, Turnbull, Adams (2012) model of Eqn. 1 in the main text. For the simulation of eastern redbud, BTA parameters with coefficients E_m = 21.88 (mmol m^{-2} s^{-1}), i_0 = 11.47 (μmol m^{-2} s^{-1}), k = 138700 (μmol m^{-2} s^{-1} mmol mol^{-1}), b = 0 (mmol mol^{-1}).

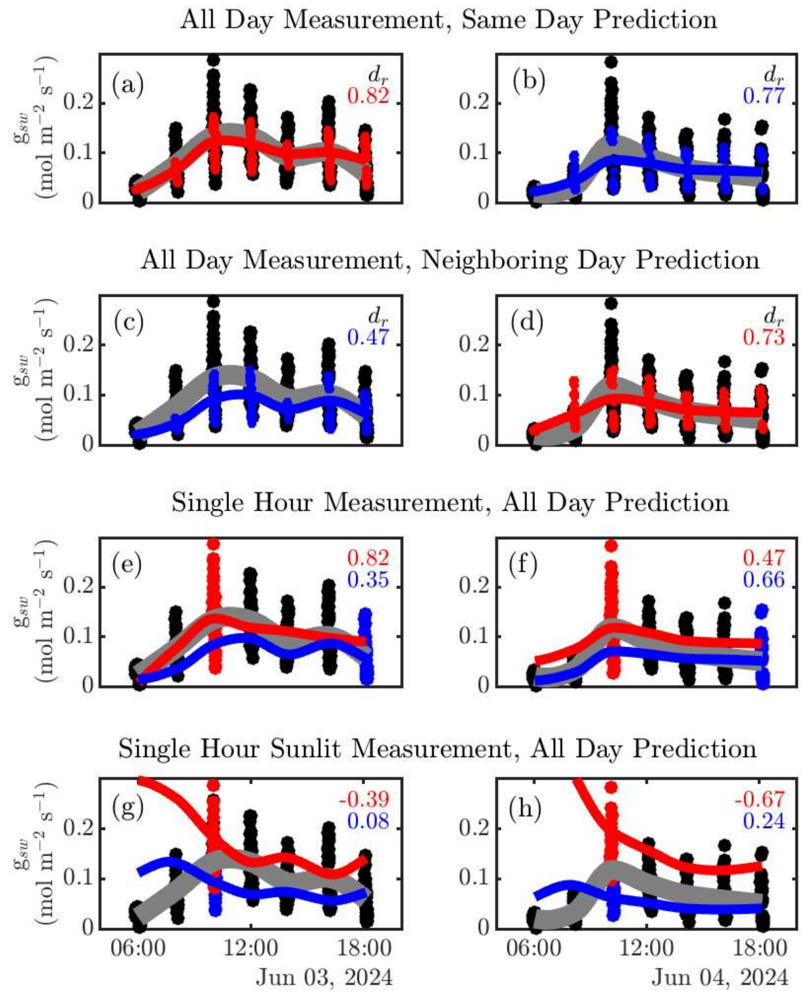

Figure S3. The representativeness of stomatal conductance model parameters calibrated from different subsets of all the data were assessed for their ability to predict whole day (or neighboring day) stomatal conductance. Leaves of an eastern redbud (Cercis canadensis) tree were sampled every two hours for two consecutive days. Subplots (a) and (b) use all the representative day's input to predict that day (interpolation), with the first day in red and following day in blue. Subplots (c) and (d) use opposite days data to predict current day (extrapolation). Subplots (e) and (f) use one hour's data to predict the whole day, 10:00-11:00 in red, and 18:00-19:00 in blue. Subplots (g) and (h) use only sunlit (red) and shaded (blue) leaves from 10:00-11:00 to predict the whole day. stomatal conductance model outputs (colored points in a-h) are compared to measured data (black points). Points are averaged in time to produce canopy estimates of the model (colored lines) and measured data (gray lines). Refined index of agreement (d_r) values (-1 to 1) between model and *canopy averages are displayed in the upper right corner of each plot, colored as the model line they represent the fit of.*

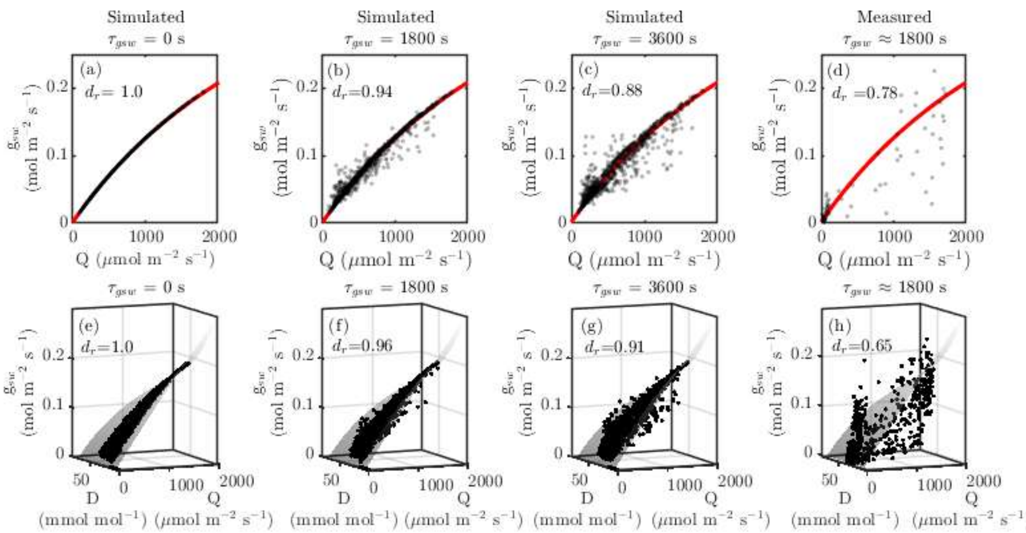

Figure S4. Simulated and measured stomatal conductance as a function of light (as Q, the absorbed leaf PPFD) and VPD (as D, the leaf to air water vapor mole fraction difference). In simulations, a stomatal time constant (τ_{gsw}) was varied to observe the effects on stomatal conductance (black points) variation about the steady-state surface from which it was generated (light gray surfaces). The top row singles out the light response at a given D of 36 mmol mol^{-1}, with data points shown across a range of 36 $\pm$ 0.25 in the simulated cases, and $\pm$ 3 in the measured case. Willmott's refined index of agreement, d_r, was used to indicate model agreement (-1 to 1) to measured and simulated points in the top left of each panel.

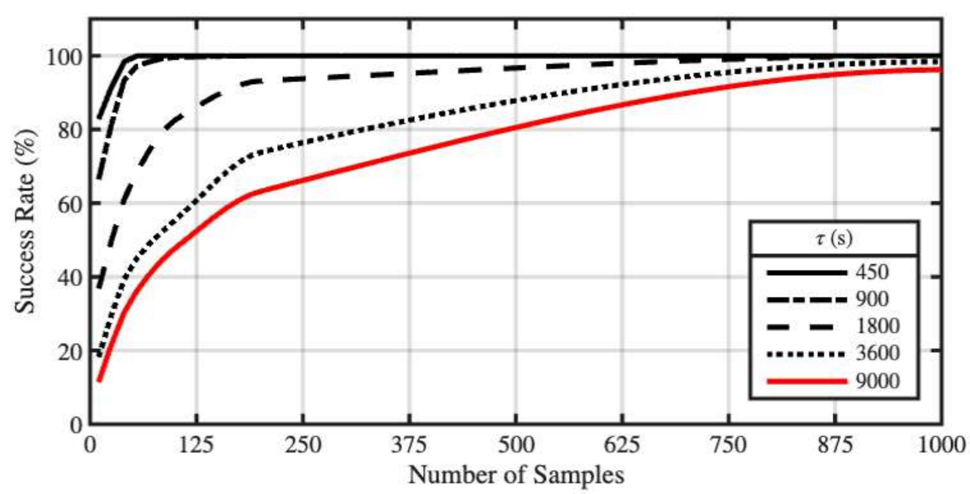

Figure S5. Slower stomatal kinetics requires more survey samples to recover steady-state stomatal conductance relationships to environmental conditions. A statistical power *analysis performed on simulated data with known stomatal model parameters and different stomatal time constants (τ) shows that the success rate of recovering true model parameters decreases with increased τ. Thus for the same success rate, more samples are needed. Here, we show the success rates for a relative error of 5% from known stomatal parameters.*

Notes S4. Rescaling of steady-state fits with survey statistics

Survey measurements have the potential to capture a lot of leaf-to-leaf physiological variation in a short of amount of time but non-steady-state, while steady-state response curves capture a very detailed response shape but take much longer to complete. Thus, only a limited set of leaves can be measured for steady-state responses in a reasonable amount of time. One approach to model the range of variation but maintain a one-to-one steady-state mapping and observed response shape is to rescale the response curves using survey statistics.

Each steady-state stomatal conductance, $g_{sw,ss,i}$ for all i data points, can be rescaled using the following transformation prior to model fitting:

$$g_{sw,ss,i} = g_{sw,ss,i} \cdot \frac{\text{percentile}\left(G_{sw,nss}, p\right)}{\max\left(G_{sw,ss}\right)} , \tag{10}$$

where $\text{percentile}(G_{sw,nss}, p)$ returns the p-th percentile of the set of non-steady-state stomatal conductance, $G_{sw,nss}$, and $\max(G_{sw,ss})$ returns the maximum of the set of steady-state stomatal conductance data, $G_{sw,ss}$. A rescaling to the 98th percentile is shown in Figure 5 in the main text, but many other statistics may be considered. For most applications it would make sense to consider the survey points within some range of Q and D that maximum stomatal conductance occurred within among the steady-state measurements, assuming those were taken prior – generally, this would occur near maximum Q and minimal D. The steady-state maximum stomatal conductance for the data shown here was measured at 2000 μmol m^{-2} s^{-1} Q and around 15 mmol mol^{-1} D (Fig. 5 in the main text).

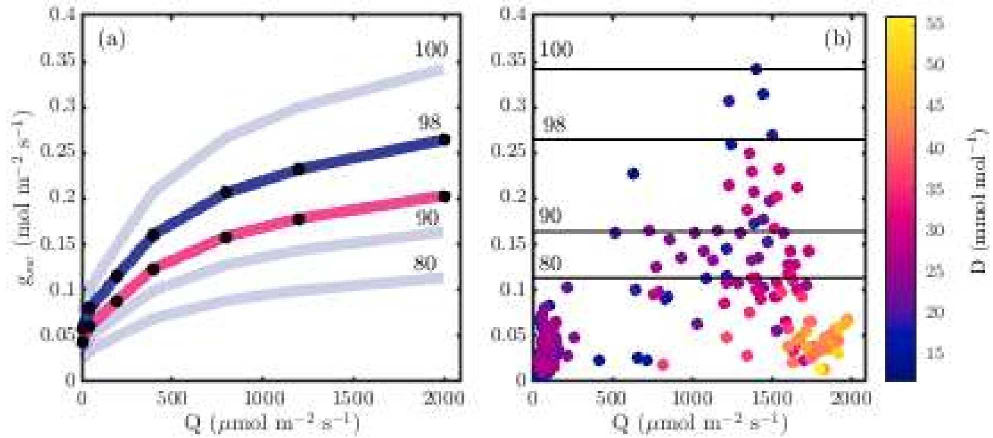

Figure S6. An example of rescaling steady-state stomatal conductance with survey statistics. A steady-state stomatal light response often takes hours to produce for one single leaf, limiting its ability to provide confidence in representativeness for the many leaves of a plant canopy. In (a), a measured light response (pink) was rescaled (blue) using statistics derived from non-steady-state point measurements in (b). Percentiles are marked in both subplots, and the 98th percentile used here to rescale the steady-state response, but many different statistics could be used depending on application.

References

Bailey, B.N., 2018. A reverse ray-tracing method for modelling the net radiative flux in leaf-resolving plant canopy simulations. Ecological Modelling 368, 233–245.

Bailey, B.N., 2019. Helios: A scalable 3D plant and environmental biophysical modelling framework. Frontiers in Plant Science 10, 1185.

Bernacchi, C., Singsaas, E., Pimentel, C., Portis Jr, A., Long, S.P., 2001. Improved temperature response functions for models of rubisco-limited photosynthesis. Plant, Cell & Environment 24, 253–259.

Buckley, T.N., Frehner, E.H., Bailey, B.N., 2023. Kinetic factors of physiology and the dynamic light environment influence the economic landscape of short-term hydraulic risk. New Phytologist 238, 529–548.

Buckley, T.N., Turnbull, T.L., Adams, M.A., 2012. Simple models for stomatal conductance derived from a process model: Cross-validation against sap flux data. Plant, Cell & Environment. 35, 1647–1662.

Farquhar, G.D., von Caemmerer, S., Berry, J.A., 1980. A biochemical model of photosynthetic CO_2 assimilation in leaves of C_3 species. Planta 149, 78–90.

Kustas, W.P., Norman, J.M., 1999. Evaluation of soil and vegetation heat flux predictions using a simple twosource *model with radiometric temperatures for partial canopy cover. Agricultural and Forest Meteorology 94, 13–29.*

Lei, T., Rizzo, K.T., Bailey, B.N., 2025. PhoTorch: a robust and generalized biochemical photosynthesis model fitting package based on PyTorch. Photosynthesis Research 163, 21.

Sharkey, T.D., Bernacchi, C.J., Farquhar, G.D., Singsaas, E.L., 2007. Fitting photosynthetic carbon dioxide response curves for C_3 leaves. Plant, Cell & Environment 30, 1035–1040.

Tetens, O., 1930. Uber einige meteorologische Begriffe. Z. Geophys 6, 297–309.